Dalton Transactions

Accepted Manuscript

ROYAL SOCIETY OF CHEMISTRY

www.rsc.org/dalton

Cite this: DOI: 10.1039/c0xx00000x

www.rsc.org/xxxxxx

ARTICLE TYPE

Cluster-controlled dimerisation in supramolecular ruthenium photosensitizer-polyoxometalate systems

Kirsten Heussner[a,b], Katrin Peuntinger[b], Nils Rockstroh[b], Sven Rau[a]* and Carsten Streb[a]*

Received (in XXX, XXX) Xth XXXXXXXXX 20XX, Accepted Xth XXXXXXXXX 20XX
DOI: 10.1039/b000000x

A supramolecular reaction system is reported where a labile molecular metal oxide cluster enables the unprecedented dimerisation of ruthenium photosensitizers $[Ru(L)_2(tmbiH_2)]^{2+}$ (L = 4,4'-di-*tert*-butyl-2,2'-bipyridine (**1a**) or 2,2'-bipyridine (**1b**); $tmbiH_2$ = 5,5',6,6'-tetramethyl-2,2'-bibenzimidazole). In the presence of $[Mo_8O_{26}]^{4-}$ clusters (**2**) the dimerisation is triggered by the *in-situ* conversion of $[Mo_8O_{26}]^{4-}$ to $[Mo_6O_{19}]^{2-}$which results in the release of hydroxide ions. Simultaneous deprotonation of the pH-sensitive $tmbiH_2$-ligands starts the dimerisation, resulting in the formation of the dinuclear complex $[(Ru(L)_2)_2(tmbi)]^{2+}$ (L = 4,4'-di-*tert*-butyl-2,2'-bipyridine (**3**) or 2,2'-bipyridine (**4**)). The dimerisation reaction can be suppressed when **2** is replaced by a stable polyoxomolybdate cluster, $[Mo_5O_{15}(PhPO_3)_2]^{4-}$ (**5**) and the reaction between **1a** and **5** leads to the formation of hydrogen-bonded supramolecular aggregates **6**. The solution and solid-state interactions in these systems were investigated using a range of spectroscopic and crystallographic techniques and compounds **3**, **4** and **6** were characterized using single-crystal XRD.

Introduction

Over the last decades, sustainable energy research has been driven by the ultimate goal of replacing fossile fuels with solar light-based energy conversion and energy storage systems.[1] Using this approach, a key concept is the efficient absorption of solar light in the visible region where the majority of light energy is available at the Earth surface.[2] Many key technologies such as dye-sensitized solar cells (DSSCs)[3] and photocatalytic water oxidation catalysts (WOCs)[4] employ photosensitizers based on $[Ru(bpy)_3]^{2+}$ (bpy = 2,2'-bipyridine)[5] with the aim of maximizing the amount of sunlight absorbed. Ruthenium-based coordination compounds are particularly suited for this task as they show maximum absorption in the mid-visible region and form long-lived photoexcited states with unusual redox properties which is crucial for efficient charge-separation and subsequent electron transfer reactions.[6] Under operative conditions in DSSCs or WOCs, the photoexcited ruthenium complex undergoes an electron transfer to an electron accepting unit to give $[Ru(bpy)_3]^{3+}$. This oxidized species is subsequently reduced to the original $[Ru(bpy)_3]^{2+}$ by an outer-sphere electron transfer from an electron donor. Although the principal mode of action of ruthenium-based photosentizers in DSSC or WOC systems is well understood, little is known about the intermolecular interactions which allow the electron and energy transfer to occur, in particular in WOCs.[3] However, understanding the intermolecular mechanisms which allow the photosensitizer to interact with other reagents in solution are a vital prerequisite for the design of high-efficiency light conversion systems.[7]

In order to address this challenge, we have recently developed a supramolecular system which can serve as a model to study the intermolecular interactions between ruthenium photosensitizers and metal oxide surfaces.[8] To achieve this, a functionalized photosensitizer, $[Ru(tbbpy)_2(biH_2)]^{2+}$ (tbbpy = 4,4'-di-*tert*-butyl-2,2'-bipyridine; biH_2 = 2,2'-biimidazole)[9] was combined with a molecular metal oxide cluster[10] $[\beta\text{-}Mo_8O_{26}]^{4-}$ and it was shown by a range of techniques that stable, supramolecular aggregates are formed in the solid state and in solution through hydrogen-bonded interactions between the biH_2 ligand and the oxo ligands of the molybdate cluster. In addition, it was demonstrated that the aggregation process is dynamic and can be controlled by the deliberate addition of ion-pairing reagents which result in the de-aggregation of the photosensitizer/metal oxide aggregates.

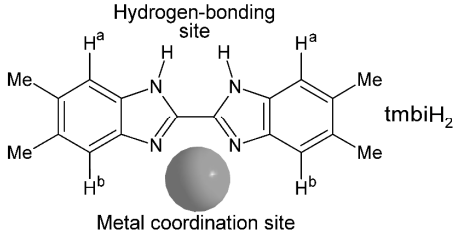

Scheme 1 Structure and interaction sites of the 5,5',6,6'-tetramethyl-2,2'-bibenzimidazole ($tmbiH_2$) ligand.

To develop this system further, we were interested in using sterically more demanding photosensitizers as it had previously been shown that steric effects can cause large

changes to the intermolecular photosensitizer-metal oxide interactions.[11] In the present study, we replaced the original biH_2 ligand on the Ru complex with the bulky organic ligand 5,5',6,6'-tetramethyl-2,2'-bibenzimidazole (hereafter: $tmbiH_2$), see Scheme 1.[12, 13]

Experimental

Materials and Methods

All chemicals were purchased from Sigma Aldrich or ACROS and were of reagent grade. Solvents used were of p.a. grade unless stated otherwise. Chemicals and solvents were used without further purification unless stated otherwise. $[Ru(tbbpy)_2(tmbiH_2)](PF_6)_2$ (**1a**$(PF_6)_2$),[13] $[Ru(bpy)_2(tmbiH_2)](PF_6)_2$[13] (**1b**$(PF_6)_2$) and $(TBA)_4[Mo_8O_{26}]$[8] ($(TBA)_4$**2**; TBA = tetra-*n*-butylammonium) were prepared as described in the literature. Product purity was confirmed using elemental analysis, ^{1}H-NMR-, UV-Vis- and FT-IR spectroscopy.

Synthetic section

Synthesis of compound 3: $[Ru(tbbpy)_2(tmbiH_2)](PF_6)_2$ (51 mg, 41.9 µmol) was dissolved in 10 ml DMF. $(TBA)_4[Mo_8O_{26}]$ (66 mg, 30.8 µmol) was dissolved in 10 ml DMF. The two clear solutions were mixed and 2 ml deionized water and 0.5 ml MeOH were added. The reaction mixture was heated to 60 ˚C for 3 days, cooled to room temperature and setup for crystallization by diffusion of ethyl acetate. After a few days, compound **3** was obtained as a dark, microcrystalline product. In order to obtain crystals suitable for single-crystal XRD, the reaction was conducted as described above without heating. Diffusion of ethyl acetate into the reaction mixture gave single crystals of compound **3**. The crystalline product was filtered off, washed twice with ethyl acetate and dried in a desiccator. Yield: 15.2 mg (5.68 µmol, 27.8 % based on Ru). Elemental analysis (dried material) for $C_{90}H_{112}Mo_6N_{12}O_{19}Ru_2$ in wt.-% (calcd.): C 44.38 (44.23); H 5.00 (4.62); N 6.33 (6.88).Characteristic IR bands (in cm^{-1}): 3482 (s), 2972 (s), 1619 (s), 1543 (m), 1482 (m), 1415 (m), 1385 (s), 1254 (w), 1133 (w), 1033 (w), 949 (s), 919 (s), 852 (m), 808 (m), 719 (m), 668 (s).

Synthesis of compound 4: $[Ru(bpy)_2(tmbiH_2)](PF_6)_2$ (25 mg, 25.3 µmol) was dissolved in 6 ml DMF. $(TBA)_4[Mo_8O_{26}]$ (32 mg, 15.5 µmol) was dissolved in 4 ml DMF. The two clear solutions were mixed and 0.5 ml deionized water was added. The reaction mixture was stirred at room temperature for 20 h and set up for crystallization by diffusion of ethyl acetate. After *ca.* 3 weeks, single crystals of compound **4** were obtained. The product was filtered off, washed with ethyl acetate and dried under vacuum. Yield: 7.9 mg (3.69 µmol, 16.9 % based on Ru). Elemental analysis (dried material) for $C_{58}H_{48}Mo_6N_{12}O_{19}Ru_2$ in wt.-% (calcd.): C 35.48 (34.91), H 2.48 (2.43), N 8.13 (8.43). Characteristic IR bands (in cm^{-1}): 3425 (m,b), 2899 (m), 1612 (s), 1532 (w), 1453 (m), 1384 (s), 948 (s), 912 (s), 849 (m), 802 (m), 724 (s), 687 (s).

Synthesis of compound 5 The synthesis of the tetra-*n*-butylammonium (TBA) salt of **5** is an adaptation of a reported synthesis which originally gave the ammonium salt.[14] $(NH_4)_6[Mo_7O_{24}]$ x 4 H_2O (10.8 g (8.88 mmol) is dissolved in 60 ml deionized water and an aqueous ammonia solution (25 %, 3.3 ml) is added. To this, phenylphosphonic acid (4.25 g, 26.88 mmol) is added. The solution pH is set to 4.7 using aqueous HCl (6 M). TBABr (15.8 g, 49.0 mmol) is dissolved in 40 ml deionized water. The solution pH is set to 3.1 using aqueous HCl (6 M). Both solutions are mixed and instantly a white precipitate is formed. The pH of the vigorously stirred suspension is set to 4.7 (HCl, 6 M). The precipitate is removed by centrifugation, washed five times with 30 ml portions of deionized water and four times with 30 ml portions of absolute ethanol. The product is dried under vacuum. Yield: 5.33 g (2.48 mmol; 20.3 % based on Mo). Elemental analysis (dried material) for $C_{76}H_{170}Mo_5N_4O_{29}P_2$ in wt.-% (calcd.): C 42.15 (42.54); H 7.71 (7.99); N 2.52 (2.61). Characteristic IR bands (in cm^{-1}): 3470 (s, b), 3055 (m), 2965 (vs), 2876 (vs), 2365 (s), 1653 (m), 1485 (vs), 1437 (m), 1383 (m), 1150 (vs), 1142 (vs), 1123 (vs), 1053 (vs), 984 (vs), 963 (vs), 936 (vs), 924 (vs), 754 (vs), 723 (vs).

Synthesis of compound 6: $(TBA)_4[Mo_5O_{15}(PhPO_3)_2]$ (20.8 mg, 9.5 µmol) was dissolved in 3 ml DMF. $[Ru(tbbpy)_2(tmbiH_2)](PF_6)_2$ (23.4 mg, 19.2 µmol) was dissolved in 3 ml DMF and both solutions were mixed and 0.5 ml deionized water was added. The solution was stirred at rt for 20 h. Single crystals of **6** were obtained by diffusion of diethyl ether into the reaction mixture. After *ca.* 4 weeks, the crystals were filtered off, washed with diethyl ether and dried under vacuum. Yield: 3.7 mg (1.59 µmol, 15.7 % based on Mo). Elemental analysis (dried material) for $C_{82}H_{109}Mo_5N_{14}O_{25}P_2Ru$ in wt.-% (calcd.): C 43.10 (42.21), H 4.79 (4.70), N 8.21 (8.40). Characteristic IR bands (in cm^{-1}): 3358 (m,b), 2969 (m), 1622 (m), 1124 (s), 1095 (s), 954 (s), 908 (s), 862 (m), 754 (m), 694 (m).

Crystallographic section

Suitable single crystals of the respective compound were grown and mounted onto the end of a thin glass fiber using Fomblin oil. X-ray diffraction intensity data were measured at 150 K on a Nonius Kappa CCD diffractometer [λ(Mo-K_α) = 0.71073 Å] equipped with a graphite monochromator or at 100 K on a Bruker APEX II CCD diffractometer [λ(Mo-K_α) = 0.71073 Å] equipped with a graphite monochromator. Structure solution and refinement was carried out using the SHELX-97 package[15] *via* WinGX.[16] Corrections for incident and diffracted beam absorption effects were applied using empirical or numerical methods.[17] Structures were solved by a combination of direct methods and difference Fourier syntheses and refined against F^2 by the full-matrix least-squares technique. Diffuse solvent correction was carried out using the SQUEEZE function within Platon.[18] Crystal data, data collection parameters and refinement statistics are listed in Table 1. These data can be obtained free of charge via www.ccdc.cam.ac.uk/conts/retrieving.html or from the Cambridge Crystallographic Data Center, 12, Union Road, Cambridge CB2 1EZ; fax:(+44) 1223-336-033; or deposit@ccdc.cam.ac.uk. CCDC reference numbers 823882 (**3**), 823883 (**4**) and 823884 (**6**).

Results and discussion

We report the supramolecular interactions observed in three ruthenium photosensitizer-molybdenum oxide cluster aggregates which were investigated in solution and in the solid state using ^{1}H-NMR-spectroscopy, UV-Vis spectroscopy, single-crystal X-ray diffractometry and bond valence sum calculations. In

addition, an unusual dimerisation reaction is reported and a possible reaction mechanism is proposed which explains the metal oxide-initiated formation of dinuclear Ru-complexes. The bulky Ru-photosensitizers $[Ru(tbbpy)_2(tmbiH_2)]^{2+}$ (**1a**) and $[Ru(bpy)_2(tmbiH_2)]^{2+}$ (**1b**) were chosen, as they contain hydrogen-bonding sites on the $tmbiH_2$ ligand for interactions with the molybdate cluster surface (Scheme 1) and only differ in the bulkyness of the non-functionalized tbbpy (**1a**) and bpy (**1b**) ligands, respectively. The molybdate cluster $[\beta\text{-}Mo_8O_{26}]^{4-}$ (**2**) was employed as it had previously been shown to be a good model for anionic metal-oxide surfaces.[8] In order to gain initial information on the interactions between the Ru-photosensitizer **1a** and the molybdate cluster **2** in solution, a ^{1}H-NMR spectroscopic titration was conducted to evaluate the formation of hydrogen-bonded supramolecular aggregates of the type {**1a**·**2**}. Convenient experimental evaluation of any interactions at the hydrogen bonding site of the $tmbiH_2$ ligand in **1a** is provided by the ^{1}H-NMR signals of the proximate protons H^a and H^b, respectively as their chemical shift δ is strongly affected by the spatial proximity of hydrogen-bonded molecules, see Scheme 1.[8-10]

Table 1 Crystallographic data for compounds **3, 4** and **6**

Compound reference	Compound **3**	Compound **4**	Compound **6**
Chemical formula	$C_{102}H_{140}Mo_6N_{16}O_{23}Ru_2$	$C_{58}H_{48}Mo_6N_{12}O_{19}Ru_2$	$C_{82}H_{116}Mo_5N_{14}O_{25}P_2Ru$
Formula Mass	2736.08	1994.85	2340.60
Crystal system	Triclinic	Monoclinic	Triclinic
a/Å	13.7646(9)	23.524(5)	16.2245(13)
b/Å	15.249(2)	18.492(4)	16.8188(18)
c/Å	15.6263(7)	19.764(4)	20.5684(17)
α/°	83.004(7)	90.00	73.816(8)
β/°	86.889(5)	113.388(4)	89.370(6)
γ/°	77.038(7)	90.00	86.799(8)
Unit cell volume/Å^3	3171.3(5)	7891(3)	5381.7(8)
Temperature/K	150(2)	100(2)	150(2)
Space group	*P*-1	*C*2/*c*	*P*-1
No. of formula units per unit cell, *Z*	1	4	2
Absorption coefficient, *μ*/mm^{-1}	0.870	1.370	0.801
No. of reflections measured	68779	31653	138426
No. of independent reflections	12942	8046	21952
R_{int}	0.0631	0.0298	0.0744
Final R_1 values ($I > 2\sigma(I)$)	0.0512	0.0395	0.0438
Final $wR(F^2)$ values ($I > 2\sigma(I)$)	0.1204	0.1082	0.1011
Final R_1 values (all data)	0.0746	0.0552	0.0728
Final $wR(F^2)$ values (all data)	0.1303	0.1138	0.1109
Goodness of fit on F^2	1.048	1.056	1.075
max/min resd. electron density / e Å^{-3}	1.733 / -0.698	1.124 / -0.807	0.804 / -0.597

An initial, comparative ^{1}H-NMR titration in DMSO-d_6 at molar ratios of **1a**:**2** = 8:1 to **1a**:**2** = 1:8 was conducted and analysis of the spectroscopic data reveals that with increasing concentration of the molybdate cluster **2**, an increased upfield shift of the H^a and H^b proton signals was observed, while the remaining aromatic proton signals belonging to the $tmbiH_2$-ligand are unchanged, see Fig. 1. In detail, the chemical shift of H^a changed from δ_{Ha} = 7.66 (**1a:2** ratio 8:1) to δ_{Ha} = 7.32 (**1a:2** ratio 1:8). For H^b, the chemical shift changed from δ_{Hb} = 5.24 (**1b:2** ratio 8:1) to δ_{Hb} = 5.19 (**1b:2** ratio 1:8).

This observation is in line with our previous investigation and gives strong indication of the formation of supramolecular {**1a**·**2**} aggregates in solution.[8] In addition, the results indicate that maximum shifts are obtained at molar ratios of **1a:2** = 1:1; a further increase of the concentration of the molybdate cluster **2** does not lead to further changes of the chemical shift, suggesting that in solution, the formation of 1:1 aggregates is preferred. In order to gain structural information on the interactions between **1a** and **2**, a series of crystallization experiments were carried out. For solubility reasons, we chose to use N,N'-dimethyl formamide (DMF) as the solvent, whereas in the initial study, dimethyl sulphoxide (DMSO) had been used. From the reagent solution, a crystalline product was obtained and single-crystal XRD analysis gave the formula $[(Ru(tbbpy)_2)_2(tmbi)][Mo_6O_{19}]$ x *ca.* 5 DMF (**3**).

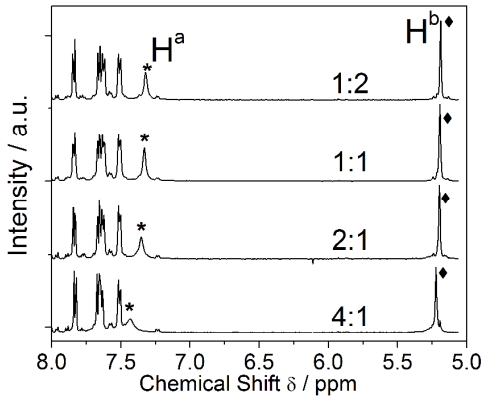

Fig. 1 ^{1}H-NMR spectroscopic titration showing the chemical shift changes of the $tmbiH_2$-based protons H^a (*) and H^b (♦) depending on the molar ratios of **1a**:**2** (shown here: 4:1⟶1:2). Solvent: DMSO- d_6. For complete titration see ESI, Fig. S5.

Structural analysis of **3** shows that not the expected, hydrogen-bonded aggregate between the Ru-photosensitizer **1a** and the molybdate cluster **2** was formed. Instead, two new molecular units were identified in the crystal lattice of compound **3** and structural analysis shows that under the given reaction conditions, both **1a** and **2** undergo conversion reactions, resulting in the formation of a dimeric ruthenium coordination complex, MESO-

$[(Ru(tbbpy)_2)_2(tmbi)]^{2+}$ (**3a**) and a hexanuclear molybdate cluster, $[Mo_6O_{19}]^{2-}$ (**3b**), see Fig. 2.

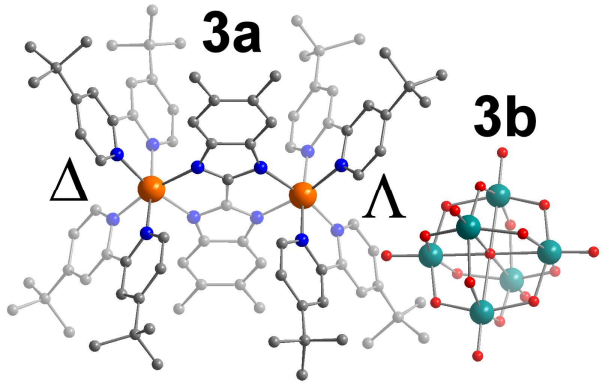

Fig. 2 Ball-and-stick representation of compound **3**, showing the Ru dimer **3a** and the hexamolybdate **3b**. Helicity-assignments for the Ru-centres are shown. Colour scheme: Mo: green, Ru: orange, O: red, N: blue, C: grey, H-atoms and solvent molecules are omitted for clarity.

It is interesting to note that starting from the racemic Δ,Λ-mixture of the Ru-precursor **1a**, only the MESO form of the Ru-dimer **3a** is observed in the solid state, suggesting that this diastereomer is preferentially formed and/or incorporated into the lattice of **3**.

In order to understand whether the unexpected formation of the MESO-Ru-dimer **3a** is linked to the formation of the hexamolybdate cluster **3b**, the reaction conditions were investigated in detail. It is known from the literature that the dimeric Ru complex **3a** is typically formed by the complexation of two $[Ru(tbbpy)_2L_2]^{2+}$ units (L = weak ligand, e.g. Cl^-) to one $tmbiH_2$ ligand under basic conditions which allow full deprotonation of the $tmbiH_2$ ligand, see Scheme 2.[12,13]

$$[Ru(tbbpy)_2L_2] + tmbiH_2 \xrightarrow[-2\,L^-,\,-2\,H^+]{base} [(Ru(tbbpy)_2)_2(tmbi)]^{2+}$$

Scheme 2 Typical formation conditions for the Ru-dimer **3a** reported in the literature. [12, 13] N. B. in the synthesis presented here, no Ru-complexes with labile ligands L are present and the formation of the dimer **3a** must be initiated by the removal of a $tmbiH_2$-ligand from a Ru complex.

However, under the given reaction conditions, this reaction pattern cannot be adopted as all Ru centres are coordinated by chelating N-donor ligands (tbbpy and $tmbiH_2$, respectively) which are kinetically inert and do not exchange in solution.[12, 13] In addition, the formation of the dimer **3a** starting from **1a** requires the twofold deprotonation of a $tmbiH_2$ ligand to create the complexation site for the second Ru centre.

In order to understand whether this initial deprotonation step could be linked to the formation of the molybdate cluster **3b**, the **2** → **3b** cluster conversion was investigated in detail. It was hypothesized that the octamolybdate-to-hexamolybdate conversion does not require the presence of the Ru complex **1a** but is caused by the intrinsic lability of the $[Mo_8O_{26}]^{4-}$ unit **2** in the chosen solvent DMF, so that the cluster undergoes a spontaneous condensation reaction, resulting in the formation of the $[Mo_6O_{19}]^{2-}$ unit **3b**. To verify this hypothesis experimentally, a sample of $(TBA)_4[Mo_8O_{26}]$ was dissolved in DMF and the **2** → **3b** conversion was followed UV-Vis spectroscopically by monitoring the changes in absorbance at λ = 321 nm. This experimental approach is feasible as both the octamolybdate and the hexamolybdate cluster show characteristic UV-Vis absorption signals, see Fig. 3, inset. The time-dependent UV-Vis spectroscopic analysis shows that the cluster conversion of **2** → **3b** indeed occurs in the absence of the ruthenium complex and the formation of the hexamolybdate **3b** follows a pseudo first order kinetics. In addition, it was observed that the **2** → **3b** cluster conversion reaches a plateau after *ca.* 40 h, see Fig. 3.

It is interesting to note that the conversion between the octamolybdate **2** and the hexamolybdate **3b** seems to be strongly dependent on the given reaction conditions: recently, a detailed ESI mass-spectrometric study was conducted[19] which showed that in the presence of methanol $[Mo_6O_{19}]^{2-}$ (**3b**) undergoes a conversion to $[Mo_8O_{26}]^{4-}$ (**2**) which represents the exact reversion of the **2** to **3a** reaction reported here.

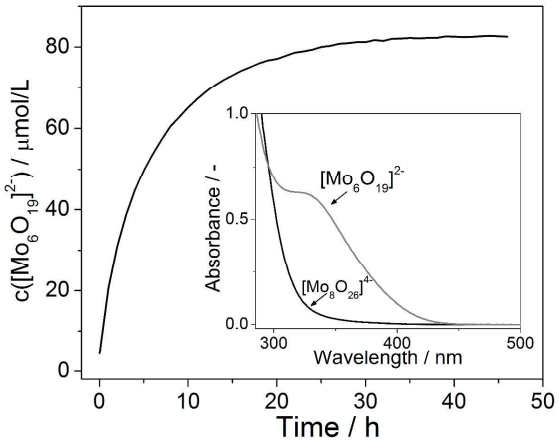

Fig. 3 Time-dependent UV-Vis spectroscopic monitoring of the conversion of $[Mo_8O_{26}]^{4-}$ (**2**) to $[Mo_6O_{19}]^{2-}$(**3b**) in DMF. Inset: UV-Vis absorption spectra of **2** (black) and **3b** (grey) in DMF.

Closer inspection of the proposed formation of the hexamolybdate **3b** shows that the cluster conversion is accompanied by the formal loss of two oxo ligands which in the presence of water (see experimental section) are released as hydroxide ions, see Scheme 3.

$$3\,[Mo_8O_{26}]^{4-} + 2\,H_2O \xrightarrow{DMF} 4\,[Mo_6O_{19}]^{2-} + 4\,OH^-$$

Scheme 3 Condensation reaction resulting in the conversion of $[Mo_8O_{26}]^{4-}$ (**2**) to $[Mo_6O_{19}]^{2-}$ (**3b**)

As the release of hydroxide ions during the conversion of $[Mo_8O_{26}]^{4-}$ to $[Mo_6O_{19}]^{2-}$ might help to explain the formation of the Ru-dimer **3a**, a preparative-scale cluster conversion experiment was conducted in order to monitor the pH value of the solution as a function of time. It was shown that with increasing $[Mo_6O_{19}]^{2-}$ formation, the basicity of the solution is increased and the pH value of the hydrolyzed solution is raised from pH = 4.46 (t = 0 h) to pH = 4.84 (t = 68 h) for [**2**] = 4.01 mM, thereby confirming the release of hydroxide ions into the reaction medium, see Fig. 4. In addition, the time-dependent increase in pH value closely resembles the characteristics of the cluster conversion measured by UV-Vis spectroscopy (Fig. 3), thereby suggesting that both processes are indeed connected.

Based on these observations, a mechanism for the first steps of the formation of compound **3** can be suggested: in the presence of the diprotonated Ru-precursor **1a**, the octamolybdate cluster **2**

undergoes a conversion reaction resulting in the formation of the hexamolybdate cluster **3b** and in the liberation of hydroxide ions. The increased basicity of the solution results in the deprotonation of **1a**, thereby creating a vacant complexation site which is a prerequisite for the formation of the Ru-dimer **3a**.

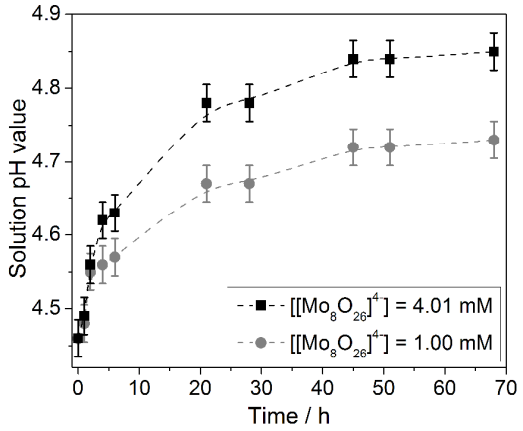

Fig. 4 Time-dependent measurement of the solution pH value during the $[Mo_8O_{26}]^{4-}$ to $[Mo_6O_{19}]^{2-}$ conversion, measured at two $[Mo_8O_{26}]^{4-}$ concentrations. For experimental details see ESI.

To gain more insight into the following reaction steps, a long-term ^{1}H-NMR-spectroscopic study was conducted where the experimental conditions of the formation of **3** were replicated using deuterated DMF-d_7 as solvent. Based on previous studies, it was known that the conversion of the monomeric complex **1a** to the dinuclear unit **3a** results in distinct changes of the signal pattern in the ^{1}H-NMR spectrum.[12, 13] However, after a period of several weeks, no change in the ^{1}H-NMR spectrum of the reaction solution was observed. Instead, an insoluble precipitate was formed and elemental analysis suggests that this precipitate corresponds to the expected composition of compound **3**. Comparative studies on the crystalline material of **3** obtained through the standard preparative route shows that **3** is indeed virtually insoluble in DMF. Therefore, it can be suggested that upon formation of the dimer **3a** under experimental conditions, precipitation or crystallization of **3** starts instantly and the solution concentration of the dimeric unit **3a** remains below the ^{1}H-NMR detection limit.

Although this study does not fully explain the final steps in the formation of the Ru-dimer **3a**, it clearly demonstrates that the presence of a molybdate species is required for the dimerisation to occur: From previous studies it is known that the monomeric Ru-unit **1a** can be kept in solution for a prolonged period of time under highly basic conditions without undergoing a dimerisation reaction.[12, 13] One possible scenario which would explain this unique reaction pattern would be the replacement of a $tmbiH_2$-ligand on **1a** by a reactive molybdate species $\{Mo_xO_y\}$ and subsequent transfer of this Ru-molybdate species to a deprotonated $[Ru(tbbpy)_2(tmbi)]$ group resulting in the formation of $[(Ru(tbbpy)_2)_2(tmbi)]^{2+}$. This hypothesis is further substantiated by a recent literature report which shows that in the **3b** → **2** conversion a range of reactive dinuclear to tetranuclear molybdate fragments of the type $\{Mo_xO_y\}^{n-}$ are observed.[19] These fragments could potentially undergo the proposed ligand exchange reaction and allow us to suggest a tentative reaction mechanism, see Scheme 4. However, it should be noted that further studies are required to fully confirm the proposed reaction scheme.

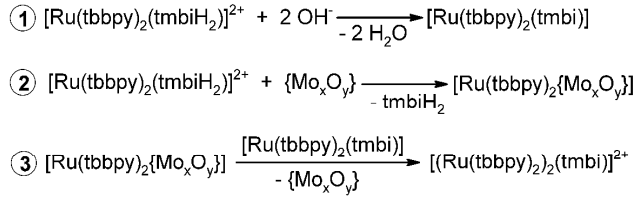

Scheme 4 Proposed formation mechanism of the Ru-dimer $[(Ru(tbbpy)_2)_2(tmbi)]^{2+}$ (**3a**). Step 1: Cluster-induced $tmbiH_2$-deprotonation. Step 2: Ligand exchange reaction (replacement of a $tmbiH_2$-ligand by a molybdate fragment). Step 3: Dimerisation reaction and loss of the molybdate fragment.

In order to understand whether the dimer formation is unique to the system employed in the synthesis of compound **3** or whether this cluster-induced dimerization might be more generally applicable, a similar Ru-system was studied where the original Ru-photosensitizer $[Ru(tbbpy)_2(tmbiH_2)]^{2+}$ **1a** was exchanged for the structural analogue $[Ru(bpy)_2(tmbiH_2)]^{2+}$ (**1b**) differing only in the peripheral substitution pattern at the bipyridine ligands.

Initial ^{1}H-NMR-spectroscopic titration experiments which were performed under similar conditions as for compound **3** showed that for the proximate probe protons H^a and H^b, significant upfield shifts were observed when the molar ratio of **1b**:**2** was increased from **1b**:**2** = 8:1 to 1:8, see Fig 5. The observed trends were very similar to the initial NMR study of the interactions between **1a** and **2**. In detail, the chemical shift of H^a changed from δ_{Ha} = 7.50 (**1b:2** ratio 8:1) to δ_{Ha} = 7.25 (**1b:2** ratio 1:8). For H^b, the chemical shift changed from δ_{Hb} = 5.17 (**1b:2** ratio 8:1) to δ_{Hb} = 5.09 (**1b:2** ratio 1:8).

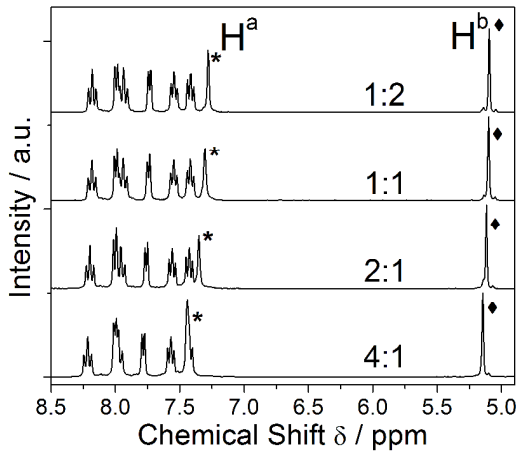

Fig. 5 ^{1}H-NMR spectroscopic titration showing the chemical shift changes of the $tmbiH_2$-based protons H^a (*) and H^b (♦) depending on the molar ratios of **1b**:**2** (shown here: 4:1⟶1:2). Solvent: DMSO- d_6. For complete titration see ESI, Fig. S6.

Further, a set of crystallization experiments was carried out to obtain crystallographic evidence of any dimerization reactions. The original experimental conditions used in the synthesis of **3** were closely followed to maximise the potential for dimerisation reactions. A crystalline product was isolated and single-crystal X-ray diffraction gave the formula $[(Ru(bpy)_2)_2(tmbi)][Mo_6O_{19}]$ x

ca. 4 DMF (**4**). Structural analysis showed that compound **4** is an analogue of compound **3**. In **4**, dimeric MESO-$[(Ru(bpy)_2)_2(tmbi)]^{2+}$ (**4a**) cations are observed which are structurally closely related to **3a**, the only difference being the lack of the bulky *tert*-butyl groups on the bpy ligands which were present in **3a**, see Fig. 6. Charge balance in **4** is achieved by the presence of the well-known $[Mo_6O_{19}]^{2-}$ cluster which is structurally identical to the hexamolybdate unit **3b**. Based on the investigations conducted for compound **3**, a similar dimerisation mechanism can be proposed for the formation of **4a** where the Ru-dimerisation is triggered by the conversion of $[Mo_8O_{26}]^{4-}$ to $[Mo_6O_{19}]^{2-}$ and proceeds *via* a deprotonation – ligand removal route resulting in the formation of the MESO-Ru-dimer **4a** and the hexamolybdate cluster $[Mo_6O_{19}]^{2-}$.

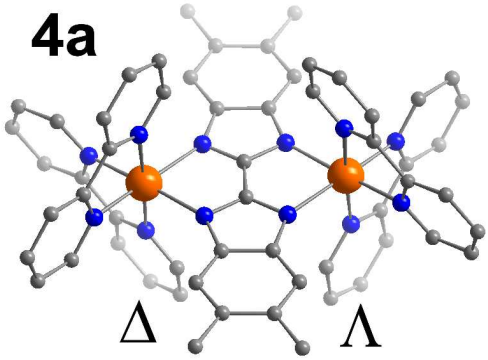

Fig. 6 Ball-and-stick representation of the MESO-Ru-dimer **4a**, giving the helicity-assignments of the Ru-centres. Colour scheme: Ru: orange, C: grey, N: blue. The $[Mo_6O_{19}]^{2-}$ cluster, H-atoms and solvent molecules were omitted for clarity.

Based on the results obtained for compounds **3** and **4** it became clear that the chosen synthetic approach would not result in stable hydrogen-bonded aggregates of monomeric Ru-photosensitizers and molybdate clusters which were the original target systems for photochemical and photophysical studies. It was hypothesized that if the octamolybdate cluster **2** is replaced with a cluster which is stable under the given operating conditions then the Ru-dimerization would be effectively prevented as the cluster-induced deprotonation and ligand removal could not proceed.

To test this hypothesis we replaced the unstable cluster unit **2** with the more stable compound **5** $[Mo_5O_{15}(PhPO_3)_2]^{4-}$.[14] **5** is comparable in size and charge to **2** but features two stabilizing, inert phenylphosphonate groups and was considered an ideal replacement for **2**. In this well-known cluster type, a five-membered molybdenum oxide ring is stabilized by two phosphonate groups *via* strong P-O-Mo coordination bonds and initial UV-Vis spectroscopic analyses showed no change of the spectral signature under the typical reaction conditions in DMF indicating an increased stability in this solvent.

In order to evaluate the long-term stability of the system, crystallization experiments were carried out using the same experimental setup that was used for compound **3** but replacing the $[Mo_8O_{26}]^{4-}$ unit **2** with the phosphonate-stabilized cluster **5**. The experiments yielded a crystalline product and single-crystal X-ray diffraction gave the formula $(Me_2NH_2)_2[Ru(tbbpy)_2(tmbiH_2)][Mo_5O_{15}(PhPO_3)_2]$ x *ca.* 4 DMF (**6**). Structural analysis showed that the experimental strategy was successful and that compound **6** features a hydrogen-bonded aggregate based on the original monomeric Ru-precursor **1a**, $[Ru(tbbpy)_2(tmbiH_2)]^{2+}$, and the molybdate cluster **5**, $[Mo_5O_{15}(PhPO_3)_2]^{4-}$. Full charge-compensation in **6** is achieved by the presence of two dimethylammonium cations formed by decomposition of the DMF solvent, see Fig. 7. The diprotonation of the $tmbiH_2$-ligand was shown by identification of the two nitrogen-bound protons from the difference fourier synthesis map.

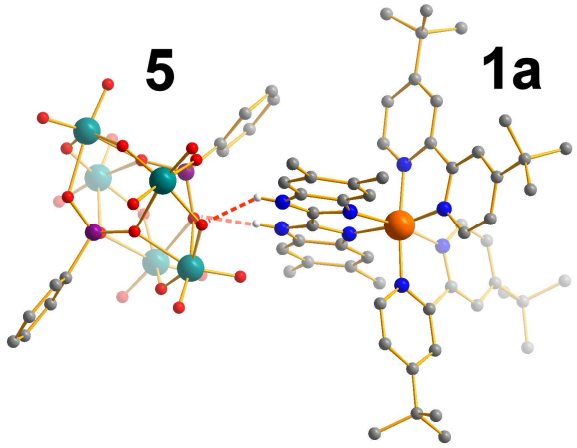

Fig. 7 Ball-and-stick representation of the hydrogen-bonded aggregate between the Ru-photosensitizer **1a** and the molybdate cluster **5** found in **6**. Colour scheme: Mo: green, Ru: orange, O: red, N: blue, C: grey, H-atoms, counter ions and solvent molecules are omitted for clarity.

In addition, bond valence sum calculations show that the molybdate cluster **5** is not protonated which further supports the protonation site assignment. In the crystal lattice of **6**, the diprotonated $tmbiH_2$-ligand forms two hydrogen-bonded interactions with the molybdate cluster **5**, resulting in the observation of two short N-H···O-Mo interactions ($d_{N...O}$ =2.843(4) Å and 2.987(5) Å, respectively). These hydrogen-bonded interactions are slightly longer compared with the values obtained our recent study of the system containing the $[Mo_8O_{26}]^{4-}$ cluster and the biimidazole-containing complex $[Ru(tbbpy)_2(biH_2)]^{2+}$.[8] This might be due to the higher steric demands of both the $tmbiH_2$ ligand in **1a** and the phenyl ligands on the molybdate cluster **5**.

To probe the existence of supramolecular interactions between the molybdate cluster **5** and the Ru-photosensitizer **1a** in solution, a ^{1}H-NMR spectroscopic titration was conducted where the molar ratios of **1a** and **5** were varied between **1a**:**5** = 8:1 to 1:8. These experiments showed the same general trend as the NMR-spectroscopic titrations for compounds **3** and **4** in that significant changes of the chemical shift of several proton species were observed. However, it became obvious that the shift patterns in this system are markedly more complex compared with the relatively straightforward shifts observed for **3** and **4**. For the probe proton H^b, an upfield shift from δ_{Hb} = 5.39 (**1a:5** ratio 8:1) to δ_{Hb} = 5.29 (**1a:5** ratio 1:1) was observed. At higher ratios of **5**, no further shift was observed, see Fig. 8.

For the probe proton H^a, an intriguing shift pattern was observed which can be separated into two regions: between ratios of **1a**:**5** = 8:1 to 4:1, the H^a signal follows the original upfield shift and a shift from δ_{Ha} = 7.53 to δ_{Ha} = 7.47 was observed.

However, for **1a**:**5** molar ratios of 2:1 to 1:8, this trend is reversed and a significant downfield shift to δ_{Ha} = 7.68 (**1a**:**5** = 1:8) was found.

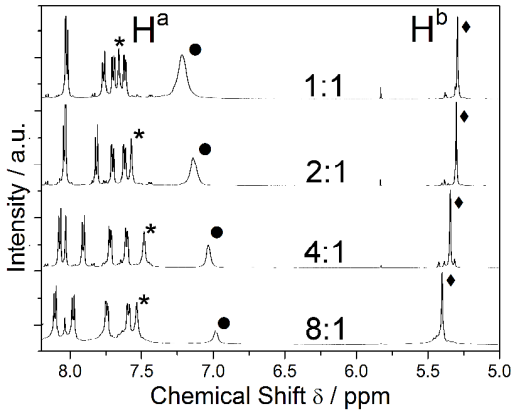

Fig. 8 ^{1}H-NMR spectroscopic titration showing the chemical shift changes of the tmbiH_2-based protons H^a (*) and H^b (♦) and the cluster-based phenyl protons (●) depending on the molar ratios of **1a**:**5** (shown here: 8:1⟶1:1). Solvent: DMF- d_7. Complete titration: see ESI, Fig. S7.

It can therefore be suggested that two types of supramolecular interactions are responsible for these shift patterns. We suggest that the upfield shifts of H^a and H^b are due to the presence of the molybdate cluster **5** at the hydrogen-bonding site of the tmbiH_2-ligand. In addition, we suggest that the downfield shift of H^a is caused by π-π interactions between the phenyl rings of the molybdate cluster **5** and the extended aromatic ligand system of the Ru-photosensitizer **1a**. This suggestion is substantiated by analysis of the crystal packing of **6** where short intermolecular contacts are observed between one phenyl ring of the molybdate unit **5** and the tmbiH_2-ligand of the Ru-complex **1a**. The minimum distance observed between the respective ring centroids is $d_{centroid}$ = 4.428 Å; the overall minimum intermolecular distance between the two rings systems is d_{min} = 3.526 Å, observed between C60 and N4 (see ESI, Fig. S4). The sensitivity of NMR-spectroscopic shifts towards π-π interactions has previously been observed for a range of aromatic coordination compounds.[20] In addition, this finding is further supported by the observation of a significant downfield shift of the cluster-based phenyl protons where the chemical shift changed from $\delta_{Hphenyl}$ = 6.97 (**1a**:**5** = 8:1) to $\delta_{Hphenyl}$ = 7.31 (**1a**:**5** = 1:8), suggesting that the phenyl protons of **5** are exposed to a changing electronic environment.

Conclusions

In conclusion, a new and unexpected synthetic approach for the dimerisation or Ru-based photosensitizers has been reported leading to the formation of MESO dinuclear complexes for two structurally related ruthenium complexes. The results were obtained while developing supramolecular model systems to study the interactions between ruthenium photosensitizers and metal oxide systems. The results demonstrate that it is crucial to understand the complex solution behaviour of supramolecular systems developed for light-harvesting applications so as to maintain a stable and reliable system under operating conditions. Mechanistically, it was shown that the dimerisation reaction occurs only in the presence of the labile molybdenum oxide cluster $[Mo_8O_{26}]^{4-}$ which under the given conditions converts into $[Mo_6O_{19}]^{2-}$ and releases hydroxide ions into the solution. It was shown that by replacing the labile molybdate cluster with a stable system, $[Mo_5O_{15}(PhPO_3)_2]^{4-}$ the dimer formation was effectively inhibited and a supramolecular complex based on monomeric Ru-photosensitizers was isolated. Strong supramolecular interactions were observed for this system when studied in solution and future work will investigate the photochemical and photophysical properties of this system in detail to identify any energy- and/or electron transfer processes between the sensitizer and the metal oxide cluster units.

Acknowledgements

This work was supported by the *Fonds der Chemischen Industrie* (FCI) through a Liebig-Fellowship (C.S.), by the *Deutsche Forschungsgemeinschaft* (DFG) through SFB 583 and by the *Deutsche Bundesstiftung Umwelt* (DBU).

Notes and references

[a] *Inorganic Chemistry I, School of Chemistry, University of Ulm, Albert-Einstein-Allee 11, 89081 Ulm, Germany, Fax: +49-731-50-23039, Tel: +49-731-50-22575, E-mail: carsten.streb@uni-ulm.de; sven.rau@uni-ulm.de; web: www.strebgroup.net*
[b] *Department of Chemistry and Pharmacy, Friedrich-Alexander-University Erlangen-Nuremberg, Egerlandstr. 1, 91058 Erlangen, Germany.*

† Electronic Supplementary Information (ESI) available: Synthetic and analytical details available. See DOI: 10.1039/b000000x/

1. (a) T. R. Cook, D. K. Dogutan, S. Y. Reece, Y. Surendranath, T. S. Teets and D. G. Nocera, *Chem Rev*, 2010, **110**, 6474; (b) N. S. Lewis and D. G. Nocera, *Proc. Natl. Acad. Sci. USA*, 2006, **103**, 15729-15735.
2. J. Forster, B. Rösner, M. M. Khusniyarov, C. Streb, *Chem. Commun.*, 2011, **47**, 3114.
3. (a) M. Grätzel, *J. Photochem. Photobiol. C*, 2003, **4**, 145; (b) A. Hagfeldt, G. Boschloo, L. C. Sun, L. Kloo and H. Pettersson, *Chem. Rev.*, 2010, **110**, 6595.
4. (a) Q. S. Yin, J. M. Tan, C. Besson, Y. V. Geletii, D. G. Musaev, A. E. Kuznetsov, Z. Luo, K. I. Hardcastle and C. L. Hill, *Science*, 2010, **328**, 342; (b) Z. Q. Huang, Z. Luo, Y. V. Geletii, J. W. Vickers, Q. Yin, D. Wu, Y. Hou, Y. Ding, J. Song, D. G. Musaev, C. L. Hill and T. Q. Lian, *J. Am. Chem. Soc.*, 2011, **133**, 2068.
5. M. Grätzel, *Philos. T. R. Soc. A*, 2007, **365**, 993.
6. (a) S. Campagna, F. Puntoriero, F. Nastasi, G. Bergamini and V. Balzani, *Top. Curr. Chem.*, 2007, **280**, 117; (b) A. Juris, V. Balzani, F. Barigelletti, S. Campagna, P. Belser and A. Vonzelewsky, *Coord. Chem. Rev.*, 1988, **84**, 85.
7. (a) T. E. Keyes, E. Gicquel, L. Guerin, R. J. Forster, V. Hultgren, A. M. Bond and A. G. Wedd, *Inorg. Chem.*, 2003, **42**, 7897; (b) N. Fay, V. M. Hultgren, A. G. Wedd, T. E. Keyes, R. J. Forster, D. Leane and A. M. Bond, *Dalton Trans.*, 2006, 4218; (c) J. J. Walsh, D. L. Long, L. Cronin, A. M. Bond, R. J. Forster and T. E. Keyes, *Dalton Trans.*, 2011, **40**, 2038.
8. K. Heussner, K. Peuntinger, N. Rockstroh, L. C. Nye, I. Ivanovic-Burmazovic, S. Rau and C. Streb, *Chem. Commun.*, 2011, DOI: 10.1039/C1CC11859E.
9. (a) C. Freys and O. S. Wenger, *Eur. J. Inorg. Chem.* **2010**, 5509; (b) S. Rau, L. Böttcher, S. Schebesta, M. Stollenz, H. Görls and D.

Walther, *Eur. J. Inorg. Chem.*, 2002, 2800; (c) S. Rau, B. Schäfer, S. Schebesta, A. Grüssing, W. Poppitz, D. Walther, M. Duati, W. R. Browne and J. G. Vos, *Eur. J. Inorg. Chem.*, 2003, 1503; (d) Y. Cui, H. J. Mo, J. C. Chen, Y. L. Niu, Y. R. Zhong, K. C. Zheng and B. H. Ye, *Inorg. Chem.*, 2007, **46**, 6427.

10. H. Abbas, C. Streb, A. L. Pickering, A. R. Neil, D. L. Long and L. Cronin, *Cryst. Growth Des.*, 2008, **8**, 635.
11. (a) N. Rockstroh, K. Peuntinger, H. Görls, D. M. Guldi, F. W. Heinemann, B. Schäfer and S. Rau, *Z. Naturforsch. B*, 2010, **65**, 281; (b) L. Ruhlmann, C. Costa-Coquelard, J. Hao, S. Jiang, C. He, L. Sun and I. Lampre, *Can. J. Chem.*, 2008, **86**, 1034.
12. (a) D. Walther, L. Böttcher, J. Blumhoff, S. Schebesta, H. Görls, K. Schmuck, S. Rau and M. Rudolph, *Eur. J. Inorg. Chem*, 2006, 2385; (b) S. Rau, M. Ruben, T. Buttner, C. Temme, S. Dautz, H. Görls, M. Rudolph, D. Walther, A. Brodkorb, M. Duati, C. O'Connor and J. G. Vos, *J. Chem. Soc.-Dalton Trans.*, 2000, 3649.
13. S. Rau, B. Schäfer, A. Grüssing, S. Schebesta, K. Lamm, J. Vieth, H. Görls, D. Walther, M. Rudolph, U. W. Grummt and E. Birkner, *Inorg. Chim. Acta*, 2004, **357**, 4496.
14. W. S. Kwak, M. T. Pope and P. R. Sethuraman, in *Inorganic Syntheses*, ed. A. P. Ginsberg, John Wiley & Sons, New York, 1990, p. 125.
15. G. M. Sheldrick, *Acta. Crystallogr. A*, 2008, **64**, 112.
16. L. J. Farrugia, *J. Appl. Cryst.*, 1999, **32**, 837.
17. (a) P. Coppens, L. Leiserowitz and D. Rabinovich, *Acta Crystallogr.*, 1965, **18**, 1035; (b) R. H. Blessing, *Acta Crystallogr. A*, 1995, **51**, 33.
18. A. L. Spek, *Acta Crystallogr. D*, 2009, **65**, 148.
19. E. F. Wilson, H. Abbas, B. J. Duncombe, C. Streb, D. L. Long and L. Cronin, *J. Am. Chem. Soc.*, 2008, **130**, 13876.
20. (a) C. E. J. Johnson and F. A. Bovey, *J. Chem. Phys.*, 1958, **29**, 1012; (b) G. P. Fulton and G. N. Lamar, *J. Am. Chem. Soc.*, 1976, **98**, 2124.

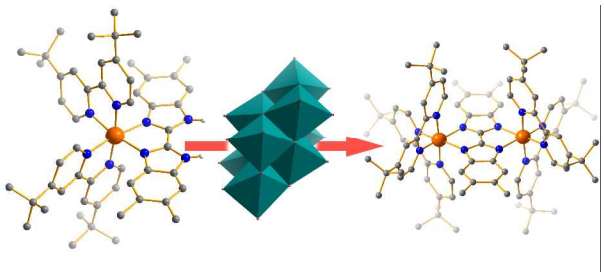

A metal oxide-triggered dimerisation reaction of Ru-photosensitizer complexes is reported which is triggered by hydroxide ions liberated during the re-arrangement of a molybdate cluster.